The superconducting critical temperature and singlet and triplet pair functions of superconductor/normal-metal/ferromagnet trilayers

Nayoung Lee and Han-Yong Choi*
Department of Physics and Institute for Basic Science Research, SungKyunKwan University, Suwon 440-746, Korea.

Hyeonjin Doh
Department of Physics, University of Toronto, Toronto, Ontario M5S 1A7, Canada.

K. Char
School of Physics and Astronomy and Center for Strongly Correlated Materials Research, Seoul National University, Seoul 151-742, Korea.

Hyun-Woo Lee
Department of Physics, Pohang University of Science and Technology, Pohang 790-784, Korea.

We calculate the superconducting critical temperature T_c, the singlet pair function $\Psi^+(x)$, and triplet pair function $\Psi^-(x)$ of superconductor/normal metal/ferromagnet (S/N/F) trilayers using the linearized Usadel equation near T_c. The Green's function method developed by Fominov *et al.* for the S/F bilayers is extended to the S/N/F trilayer systems. The S of the trilayers is taken to be an s-wave singlet pairing superconductor, and the S/N and N/F interfaces are modeled in terms of the interface resistances parameterized, respectively, by γ_b^{SN} and γ_b^{NF}. We present the T_c, $\Psi^+(x)$, and $\Psi^-(x)$ for typical γ_b^{SN}, γ_b^{NF}, and the exchange energy E_{ex}: (a) For a small (large) γ_b^{NF}, T_c of S/N/F trilayers, as d_N is increased, increases (decreases) on the length scale of N coherence length ξ_N with a discontinuity at $d_N = 0$ due to a boundary condition mismatch. (b) $T_c(d_F)$ shows a non-monotonic behavior like S/F bilayers with a weakened shallow dip. (c) The odd frequency triplet component $\Psi^-(x)$, induced by E_{ex} and proximity effects, has a maximum near the N/F interface and decreases on the length scale ξ_{ex} in F. It also penetrates into N and S regions on the length scale ξ_N and ξ_S, respectively. Based on these results we make comments on the experimental observation of the odd triplet components and the recent T_c measurements in Nb/Au/CoFe trilayer systems.

PACS numbers: PACS: 74.45.+c, 74.78.Fk, 74.25.Ha, 74.20.Rp

I. INTRODUCTION AND MOTIVATION

When different states of matter are in contact, one affects the other over the coherence length ξ, which is referred to as the proximity effects.[1,2,3,4] For instance, when a superconductor (S) and a normal metal (N) are in contact as in an S/N bilayer, the singlet pair function $\Psi^+(x) \sim \langle \phi_\uparrow(x)\phi_\downarrow(x)\rangle$, where $\phi_\sigma(x)$ is the field operator of spin σ electron at the position x and $\langle\ \ \rangle$ means the thermodynamic average, penetrates into the N region and decays exponentially on the length scale of N coherence length ξ_N. For diffusive metals, $\xi_N = \sqrt{D_N/2\pi T}$ where D_N is the diffusion constant of the normal metal and T is the temperature.[1,2] Note that, however, the gap energy given by $\Delta(x) = V\Psi^+(x)$ vanishes in N because the pairing interaction $V = 0$ in the N region. The superconducting temperature T_c of an S/N bilayer as a function of N thickness d_N also decreases exponentially on the length scale of ξ_N. Here, T_c is defined with the current parallel to the interfaces. Therefore, T_c of an S/N bilayer is determined by the highest temperature at which the singlet pair function $\Psi^+(x)$ does not vanish at least at one point within the bilayer.

The proximity effects in S/F bilayers have also been studied intensively.[3,4] Like the S/N case, $\Psi^+(x)$ of an S/F bilayer decreases exponentially in the F region, and T_c decreases as the F thickness d_F is increased. Many of the interesting S/F proximity effects occur at the nanoscale range of layer thickness. The observation of these effects was made possible by the progress of fabrication technique of high quality hybrid S/F layers. The S/F proximity effects have the following differences compared with S/N: (a) The decay length scale in F, ξ_{ex}, given by $\xi_{ex} = \sqrt{D_F/E_{ex}}$, is much shorter than ξ_N because the exchange energy E_{ex} is much larger than T. (b) The pair function oscillates as well as decreases in the F region because the net momentum of a Cooper pair is non-zero in F.[5] By the same reason $T_c(d_F)$ does not monotonically decrease like S/N as d_F is increased but shows a shallow dip. The oscillation has been confirmed by the observation of the "π-state" in S/F/S Josephson junction,[6,7,8,9] where two superconductors separated by a ferromagnet of appropriate thickness can have a phase difference of π. (c) Triplet pairing component (TPC) is induced in addition to the dominant singlet pairing component (SPC).

*To whom the correspondences should be addressed: hychoi@skku.edu.

The triplet pairing is realized in ^{3}He and Sr_2RuO_4, for instance, in the form of p-wave pairing.[10] The induced TPC in S/F systems in the diffusive limit, however, is even (s-wave) in momentum but odd in frequency, referred to as odd frequency triplet pairing component (OFTPC). The OFTP was first suggested by Berezinskii in the context of ^{3}He superfluidity,[11] but it turned out that it is the p-wave triplet pairing that is realized in ^{3}He. The OFTPC is induced from s-wave SPC because time reversal symmetry is broken by the exchange field in S/F bilayers. Just like non-s-wave pairing components are induced from s-wave one when the translational symmetry is broken, OFTPC is induced in S/F bilayers from the singlet component because the time reversal symmetry is broken by the exchange field in F region. This can be seen directly from Fig. 4 where the induced TPC vanishes as $E_{ex} \to 0$.

While it is natural to expect that the characteristic length scale in F region is very short given by ξ_{ex}, it was realized that there exist long range proximity effects in S/F systems set by the long length scale of $\xi_F = \sqrt{D_F/2\pi T}$. For instance, the long range triplet pairing was suggested to understand the unexpected conductance increase of S/F structures below T_c.[12,13,14] The condition for the occurrence of the long length TPC is that the magnetization is *not* unidirectional. When the magnetization in F is unidirectional, the induced triplet pairing component has the short coherence length ξ_{ex} like the singlet one and can be represented as $S_z = 0$ component along the magnetization direction in F.[15] More explicitly, it is given by $\langle \phi_\uparrow(x,\tau)\phi_\downarrow(x) + \phi_\downarrow(x,\tau)\phi_\uparrow(x)\rangle$, where τ is the imaginary time. When the magnetization is not unidirectional, on the other hand, other triplet components with $S_z = \pm 1$ given by $\langle \phi_\uparrow(x,\tau)\phi_\uparrow(x)\rangle$ and $\langle \phi_\downarrow(x,\tau)\phi_\downarrow(x)\rangle$ are also induced because $S_z = 0$ along a spin quantization axis is not pure $S_z = 0$ but a mixture of $S_z = 0$, $+1$, and -1 along a different axis. The $S_z = \pm 1$ TPC has the long coherence length ξ_F in F because the exchange field is not pair breaking for them.

We here note the following distinctive features of the TPC which appears in S/F systems.[4] See below for more detailed discussion. (a) The S in an S/F bilayer is a conventional s-wave singlet superconductor. The exotic state of OFTPC is induced not because the S of the S/F is exotic. It is induced because of the proximity effects and the broken time reversal symmetry. (b) TPC is induced in addition to the dominant SPC, and may have short coherence length ξ_{ex} or long coherence length ξ_F. (c) TPC is even in momentum but odd in frequency. (d) The T_c of an S/F bilayer is determined by the SPC (See Eq. (9) below.), and TPC can change T_c indirectly only by changing SPC through the boundary conditions. See Sec. II in the following for detailed discussions. The OFTP is an exotic state of matter, but it has not been directly observed yet. A lot of experimental and theoretical work has focused on finding fingerprints of the OFTP correlations.[16,17] The basic idea is that one convert the short range triplet component into the long range one by controlling or inducing nonuniformity of the F magnetization direction, and observe the long length scale triplet component with appropriate experiments. Even when the exchange field is uniform in the F, the long range components are induced when the interface is spin active which causes spin flip or spin rotation.[18,19,20,21] The present formulation can be straightforwardly applied in this case too with a modified version of the boundary conditions (BC) given by Eq. (13). Recently, there was a report which strongly hints the existence of long length OFTPC in S/F/S.[16]

The superconductor-ferromagnet systems, as described above, exhibit very interesting and exotic behavior, and it will be important to understand them in a systematic way. To do that, we have theoretically studied the S/N/F trilayer systems. By varying the intervening N thickness d_N and the interface resistances between S and N and N and F, represented in terms of γ_b^{SN} and γ_b^{NF}, respectively, we can control the proximity effects in a systematic way. In this paper, the proximity effects in S/N/F trilayers are studied for T_c, SPC, and TPC. This paper is organized as follows: After this section, we present in Sec. II the generalization to S/N/F trilayers of the numerically exact Green's function method developed by Fominov *et al.*[22] for S/F bilayers. The resulting Usadel equations subject to appropriate boundary conditions are then solved self-consistently by numerical iterations for T_c, SPC, and TPC. The results will be presented in Sec. III for typical values of γ_b^{SN}, γ_b^{NF}, and E_{ex}. Based on these results, we will make some comments on the experimental observation of the odd frequency triplet components and the recent T_c measurements in Nb/Au/CoFe trilayer systems.[23] We then conclude with the summary and concluding remarks in Sec. IV. In Appendix, we collect some technical details for calculating the singlet and triplet pairing components.

II. USADEL FORMULATION

A. Usadel equation for S/N/F trilayers

We wish to understand the proximity effects in the S/N/F trilayer systems, which is schematically shown in Fig. 1. The S is a conventional s-wave singlet pairing superconductor like Nb, N is Au, Cu, or Al (above Al's T_c), and F is CoFe or Ni. Each of S, N, F is characterized by the coherence length ξ and resistivity ρ. In addition, S layer is described by superconducting critical temperature T_{c0}, and F by the exchange energy E_{ex}. The layers of thin films are in the dirty limit and we employ the dirty limit quasi-classical theory, the Usadel equation, to describe them.[24] Moreover, since we are interested in calculating the superconducting transition temperature T_c and the pair functions near $T \approx T_c$ of S/N/F, we will use the linearized Usadel equation. Near T_c, The normal Green function is $G = sgn(\omega_n)\delta_{\sigma,\sigma'}$, where σ and σ' are the spins of two electrons forming a Cooper pair, and the anomalous function is $F \to 0$. The Usadel equation is

therefore linearized with respect to F. In a general case where all four components of F are kept, F may be represented as a 2×2 matrix or a 4 component vector. In the present problem where the exchange field is uniform over the F region, only two components, SPC and short range TPC, appear in the equation and the anomalous function F may be represented as a two component vector or scalar complex function. Because we will consider long range TPC in a subsequent study where a vector representation is convenient we will formulate the present problem in terms of two component vector

$$\mathbf{F}_i(x,i\omega_n)=\begin{pmatrix} F_i^+(x,i\omega_n)\\ F_i^-(x,i\omega_n)\end{pmatrix}, \tag{1}$$

where $i=$ S, N, or F, and x is the coordinate perpendicular to the interface and the translational symmetry is assumed parallel to the interface. The superscript $\pm$ refers to the even and odd functions of the frequency.

$$F^{\pm}(x,i\omega_n)\equiv\frac{F(x,i\omega_n)\pm F(x,-i\omega_n)}{2}, \tag{2}$$

where the anomalous function F is defined by

$$F(x,i\omega_n)=-\int_0^\beta d\tau e^{i\omega_n\tau}T_\tau\langle\phi_\uparrow(x,\tau)\phi_\downarrow(x,0)\rangle, \tag{3}$$

where T_τ is the τ ordering operator. Then, $F(x,-i\omega_n)=\int_0^\beta d\tau e^{i\omega_n\tau}T_\tau\langle\phi_\downarrow(x,\tau)\phi_\uparrow(x,0)\rangle$, and the even function F^+ represents the SPC and the odd function F^- the TPC of the anomalous function. We will also use the SPC (TPC) to stand for $\Psi^+(x)$ ($\Psi^-(x)$) which is just the summation over Matsubara frequencies of $F^+(x,i\omega_n)$ ($F^-(x,i\omega_n)$) as given in Eq. (50).

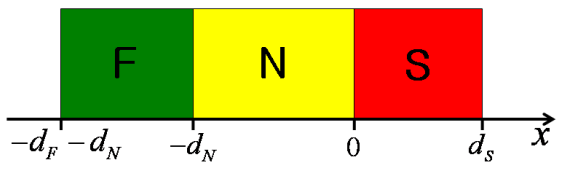

FIG. 1: Schematic drawing of an S/N/F trilayer. The coordinate x is taken as perpendicular to the interfaces.

The linearized Usadel equation near $T\approx T_c$ takes the following form:[22]

$$\xi_S^2\pi T_c\frac{\partial^2}{\partial x^2}\mathbf{F}_S(x,i\omega_n)=|\omega_n|\mathbf{F}_S(x,i\omega_n)-\mathbf{\Delta}(x),\quad(0<x<d_S), \tag{4}$$

$$\xi_N^2\pi T_c\frac{\partial^2}{\partial x^2}\mathbf{F}_N(x,i\omega_n)=|\omega_n|\mathbf{F}_N(x,i\omega_n),\quad(-d_N<x<0), \tag{5}$$

$$\xi_F^2\pi T_c\frac{\partial^2}{\partial x^2}\mathbf{F}_F(x,i\omega_n)=|\omega_n|\mathbf{F}_F(x,i\omega_n)+i\ \mathrm{sgn}\ (\omega_n)\ E_{\mathrm{ex}}\sigma_1\mathbf{F}_F(x,i\omega_n),\quad(-d_F-d_N<x<-d_N). \tag{6}$$

where $\omega_n=2\pi T(n+\frac{1}{2})$ is the Matubara frequency and σ_1 is the Pauli spin matrix. $\mathbf{\Delta}(x)=\begin{pmatrix}\Delta(x)\\0\end{pmatrix}$. Eq. (6) explicitly shows that the exchange field E_{ex} couples the SPC F_F^+ and TPC F_F^- and induces TPC from SPC. The coherence length is $\xi=\sqrt{\frac{D}{2\pi T_c}}$ in the dirty limit where D is the diffusion constant. Then,

$$\xi_S=\sqrt{\frac{D_S}{2\pi T_c}},\quad \xi_N=\sqrt{\frac{D_N}{2\pi T_c}},\quad \xi_F=\sqrt{\frac{D_F}{2\pi T_c}} \tag{7}$$

in each S, N, and F layer, as discussed in Introduction. The singlet component F_S^+ determines the gap function $\Delta(x)$

$$\Delta(x)=Vg(\epsilon_F)\pi T_c\sum_{\omega_n>0}F_S^+(x,i\omega_n), \tag{8}$$

where V and $g(\epsilon_F)$ are, respectively, the pairing interaction and the density of states per spin at the Fermi level. It satisfies the self-consistency relation

$$\Delta(x)\ln\left(\frac{T_{c0}}{T_c}\right)=\pi T_c\sum_{\omega_n}\left[\frac{\Delta(x)}{|\omega_n|}-F_S^+(x,i\omega_n)\right], \tag{9}$$

where T_c is the superconducting critical temperature of the S/N/F trilayer and T_{c0} is that of the S layer alone without the N and F layers. Eq. (9) explicitly shows that T_c is determined by the singlet component alone. The triplet components may affect T_c only by changing the singlet component through the boundary conditions discussed below.

Being a differential equation, the Usadel equation must be supplemented by boundary conditions. The appropriate BC for the Usadel equation are well established and given as follows.[25]

$$\frac{d}{dx}\mathbf{F}_F(-d_F-d_N)=0, \tag{10}$$

$$\xi_N\frac{d}{dx}\mathbf{F}_N(-d_N)-\gamma_{NF}\xi_F\frac{d}{dx}\mathbf{F}_F(-d_N)=0, \tag{11}$$

$$\xi_S\frac{d}{dx}\mathbf{F}_S(0)-\gamma_{SN}\xi_N\frac{d}{dx}\mathbf{F}_N(0)=0, \tag{12}$$

$$\mathbf{F}_N(-d_N)-\mathbf{F}_F(-d_N)=\gamma_b^{NF}\xi_F\frac{d}{dx}\mathbf{F}_F(-d_N), \tag{13}$$

$$\mathbf{F}_S(0)-\mathbf{F}_N(0)=\gamma_b^{SN}\xi_N\frac{d}{dx}\mathbf{F}_N(0), \tag{14}$$

$$\frac{d}{dx}\mathbf{F}_S(d_S)=0, \tag{15}$$

where

$$\gamma_{NF}\equiv\frac{\rho_N\xi_N}{\rho_F\xi_F},\quad \gamma_{SN}\equiv\frac{\rho_S\xi_S}{\rho_N\xi_N}. \tag{16}$$

The γ_b^{SN} and γ_b^{NF} are dimensionless quantities characterizing S/N and N/F interfaces, respectively, given by

$$\gamma_b^{NF}\equiv\frac{R_b^{NF}\mathcal{A}}{\rho_F\xi_F},\qquad \gamma_b^{SN}\equiv\frac{R_b^{SN}\mathcal{A}}{\rho_N\xi_N}, \tag{17}$$

where R_b^{NF} and R_b^{SN} are the interface resistances between N and F and S and N, respectively, and $\mathcal{A}$ is the interface area. γ_b^{SN} and γ_b^{NF} are modeled in terms of spin conserving potential barriers,[25,26] and do not introduce any spin modifying mechanism. On the other hand, the boundary of the F can be spin dependent[27] or spin active,[18,19,20,21] and the BC of Eq. (13) should be modified accordingly. The spin-active interface can induce the long range triplet components. One possible description of the spin-active interface is that the parameter γ_b^{NF} is given by a 4×4 matrix instead of a scalar with the state of Eq. (1) enlarged to a four component vector. All of the four components, two of which are the long range ones, are non-vanishing in general because they are coupled via the BC Eq. (13).

B. Boundary condition in terms of $\mathbf{F}_S$

The Usadel equation (4), (5), (6) together with the BC (10), (11), (12), (13), (14), (15) and self-consistency equation (9) forms a complete set of equations to describe an S/N/F trilayer near $T \approx T_c$. It is solved by extending the numerically exact Green's function technique developed by Fominov *et al.* for the S/F bilayers.[22,28] To utilize the technique, everything should be written in terms of $\mathbf{F}_S$ alone in the S region. The Usadel equation and the self-consistency relation are already written in terms of $\mathbf{F}_S$ alone in the S region, and the remaining task is to write the BC at $x=0$ and $x=d_S$ in terms of $\mathbf{F}_S$ only. The BC at $x=d_S$ is already given by Eq. (15), and the one at $x=0$ can be derived by writing the Usadel equation with the corresponding BC successively starting from the F to N regions. The procedure is very similar to Fominov *et al.*[22]

First, for the F region we solve the homogeneous equation (6) with BC (10) to obtain

$$\mathbf{F}_F = \begin{pmatrix} \cosh k_F(x_{NF}) & \cosh k_F^*(x_{NF}) \\ -\cosh k_F(x_{NF}) & \cosh k_F^*(x_{NF}) \end{pmatrix} \begin{pmatrix} C_F^+(i\omega_n) \\ C_F^-(i\omega_n) \end{pmatrix} \quad (18)$$

where

$$x_{NF} = x + d_N + d_F, \quad k_F = \frac{1}{\xi_F}\sqrt{\frac{|\omega_n| + iE_{ex}}{\pi T_c}}. \quad (19)$$

Note that the k_F implies another length scale ξ_{ex} much shorter than ξ_F alluded earlier. Because $E_{ex} \gg |\omega_n|$ for relevant Matsubara frequencies, one has

$$\xi_{ex} = \frac{1}{Re\,(k_F)} = \sqrt{\frac{D_F}{E_{ex}}}. \quad (20)$$

The length scale of pair function is given by ξ_{ex} in F region. From (18) we obtain

$$\xi_F \frac{d}{dx}\mathbf{F}_F(-d_N) = \hat{\mathcal{A}}_F \mathbf{F}_F(-d_N), \quad (21)$$

where

$$\hat{\mathcal{A}}_F \equiv \begin{pmatrix} \mathrm{Re}A_F & -i\mathrm{Im}A_F \\ -i\mathrm{Im}A_F & \mathrm{Re}A_F \end{pmatrix}, \quad (22)$$

$$A_F \equiv k_F\xi_F \tanh k_F d_F. \quad (23)$$

Then, utilizing the BC at $x=-d_N$ of Eq. (11) and (13), the $\mathbf{F}_N(-d_N)$ and $\frac{d}{dx}\mathbf{F}_N(-d_N)$ can be written in terms of $\mathbf{F}_F(-d_N)$ and $\frac{d}{dx}\mathbf{F}_F(-d_N)$. Then, using Eq. (21), we find

$$\xi_N \frac{d}{dx}\mathbf{F}_N(-d_N) = \hat{\mathcal{A}}_{NF}\mathbf{F}_N(-d_N), \quad (24)$$

where

$$\hat{\mathcal{A}}_{NF} \equiv \left(1 + \hat{\mathcal{A}}_F\gamma_b^{NF}\right)^{-1}\gamma_{NF}\hat{\mathcal{A}}_F. \quad (25)$$

Second, the anomalous function $\mathbf{F}_N$ in the N region described by Eq. (5) may be written as

$$\mathbf{F}_N(x,i\omega_n) = \mathbf{F}_N(-d_N)\cosh k_N(x+d_N) + \xi_N\frac{d}{dx}\mathbf{F}_N(-d_N)\frac{\sinh k_N(x+d_N)}{k_N\xi_N}, \quad (26)$$

where

$$k_N = \frac{1}{\xi_N}\sqrt{\frac{|\omega_n|}{\pi T_c}}. \quad (27)$$

Then, we use Eqs. (26) and (24) to obtain

$$\xi_N \frac{d}{dx}\mathbf{F}_N(0) = \hat{\mathcal{A}}_{NS}\mathbf{F}_N(0), \quad (28)$$

where

$$\hat{\mathcal{A}}_{NS} \equiv \left(A_N + \hat{\mathcal{A}}_{NF}\right)\left(1 + \frac{\hat{\mathcal{A}}_{NF}A_N}{k_N^2\xi_N^2}\right)^{-1}, \quad (29)$$

$$A_N = k_N\xi_N \tanh k_N d_N. \quad (30)$$

Third, using BC at $x=0$ given by Eqs. (12) and (14), and Eq. (28), we can finally obtain the BC in terms of $\mathbf{F}_S(0)$ and $\frac{d}{dx}\mathbf{F}_S(0)$ such as

$$\xi_S\frac{d\mathbf{F}_S(0)}{dx} = \hat{A}_S\mathbf{F}_S(0), \quad (31)$$

where

$$\hat{\mathcal{A}}_S \equiv \left(1 + \hat{\mathcal{A}}_{NS}\gamma_b^{SN}\right)^{-1}\gamma_{SN}\hat{\mathcal{A}}_{NS}. \quad (32)$$

Eq. (31) connects $\frac{dF_S^+(0)}{dx}$ and $\frac{dF_S^-(0)}{dx}$ with $F_S^+(0)$ and $F_S^-(0)$. But, we need the BC which connect $\frac{dF_S^+(0)}{dx}$ with $F_S^+(0)$ only to solve the Usadel equation in S region for $0 < x < d_S$ given by Eq. (4).

$$\pi T_c\xi_S^2\frac{\partial^2}{\partial x^2}F_S^+(x,i\omega_n) - |\omega_n|F_S^+(x,i\omega_n) = -\Delta(x). \quad (33)$$

We write from BC of (15)

$$F_S^-(x,i\omega_n) = C_S^-(i\omega_n)\cosh k_S(x-d_s), \tag{34}$$

where

$$k_S = \frac{1}{\xi_S}\sqrt{\frac{|\omega_n|}{\pi T_c}}. \tag{35}$$

Using this to eliminate the $F_S^-(0)$ from (31) for $\frac{dF_S^+(0)}{dx}$, we obtain

$$\xi_S \frac{dF_S^+(0)}{dx} = W(i\omega_n)F_S^+(0), \tag{36}$$

where

$$W(i\omega_n) = \gamma_{SN}\frac{A_S(\gamma_b^{SN}+ReB_{SN})+\gamma_{SN}}{A_S|\gamma_b^{SN}+B_{SN}|^2+\gamma_{SN}(\gamma_b^{SN}+ReB_{SN})}, \tag{37}$$

and A_S and B_{SN} are defined by

$$A_S = k_S\xi_S\tanh k_S d_S, \tag{38}$$

$$B_{SN} = [k_N\xi_N\tanh k_N(d_N+x_0)]^{-1} \tag{39}$$

$$\tanh k_N x_0 = \frac{1}{k_N\xi_N}\frac{\gamma_{NF}}{\gamma_b^{NF}+A_F^{-1}}. \tag{40}$$

C. Green's function method

Now, the problem is reduced to solving Eq. (33) with BC (15) and (36). To do it by the Green's function technique, one needs to solve the following source equation.[22,28]

$$\pi T_c\xi_S^2\frac{\partial^2}{\partial x^2}G(x,y) - |\omega_n|G(x,y) = -\delta(x-y), \tag{41}$$

with the BC corresponding to (36) and (15)

$$\xi_S\frac{\partial}{\partial x}G(0,y) = W(i\omega_n)G(0,y), \tag{42}$$

$$\xi_S\frac{\partial}{\partial x}G(d_S,y) = 0. \tag{43}$$

The Green's function can be constructed as follows.[28]

$$G(x,y;i\omega_n) = \frac{k_S/|\omega_n|}{\sinh k_S d_S + \frac{W(i\omega_n)}{k_S\xi_S}\cosh k_S d_S} \times \begin{cases} v_1(x)v_2(y), & 0<x<y \\ v_1(y)v_2(x), & y<x<d_S \end{cases}, \tag{44}$$

where

$$v_1(x) = \cosh k_S x + \frac{W(i\omega_n)}{k_S\xi_S}\sinh k_S x, \tag{45}$$

$$v_2(x) = \cosh k_S(x-d_S). \tag{46}$$

The solution of (33) is then

$$F_S^+(x,i\omega_n) = \int_0^{d_S} dy G(x,y;i\omega_n)\Delta(y). \tag{47}$$

The gap function $\Delta(x)$ is determined by Eq. (8).

Substituting (47) into (8) gives the self-consistency equation,

$$\Delta(x) = Vg(\epsilon_F)\pi T_c\sum_{\omega_n>0}\int_0^{d_S} dy G(x,y;i\omega_n)\Delta(y). \tag{48}$$

From this self-consistency equation, we can write down the equation for T_c with respect to T_{c0}.

$$\Delta(x)\ln\left(\frac{T_{c0}}{T_c}\right) = \int_0^{d_S} dy\ M(x,y)\Delta(y),$$
$$M(x,y) \equiv \pi T_c\sum_{\omega_n>0}\left[\frac{\delta(x-y)}{|\omega_n|} - G(x,y;i\omega_n)\right]. \tag{49}$$

The above integral equation can be reduced to an eigenvalue problem after we change the integration over y into a summation by discretization. The T_c is determined by the smallest eigenvalue of the discretized $M(x,y)$ matrix, which yields the highest T_c. One plugs an arbitrary initial T_c into the right hand side of Eq. (49) and calculates a new T_c, and iterates until the input and output are equal within a tolerance. After a convergence is reached, T_c is obtained, and the corresponding eigenvector to the smallest eigenvalue gives $\Delta(x)$. Then, the anomalous function F^+ can be obtained from Eq. (47), and the singlet and triplet pair functions $\Psi^+(x)$ and $\Psi^-(x)$ can be calculated from

$$\Psi^\pm(x) = \pi T_c\sum_{\omega_n>0}F^\pm(x,i\omega_n). \tag{50}$$

Technical details for calculating SPC and TPC are collected in Appendix.

III. RESULTS: T_c AND PAIR FUNCTIONS OF S/N/F TRILAYERS

A. Perfect interfaces

T_c of S/N/F trilayers were calculated by self-consistently solving Eq. (49) by numerical iterations. And T_c of S/N bilayers were calculated for comparison. The singlet and triplet pair functions were also calculated as detailed in Appendix. Let us first consider the ideal case of perfect interfaces with $\gamma_b^{SN} = \gamma_b^{NF} = 0$. We take $\rho_S = 15.9627\ \mu\Omega$cm, $\rho_N = 2.0\ \mu\Omega$cm, $\rho_F = 40.0\ \mu\Omega$cm, $\xi_S = 7.0$ nm, $\xi_N = 110$ nm, $\xi_F = 10.241$ nm, $E_{ex} = 1235$ K, and $T_{c0} = 7.927$ K, which are appropriate for S = 23 nm Nb, N = Au, and F = CoFe as reported in the reference[23,29]. Recall that the condition $E_{ex}\tau \ll 1$ should be satisfied for the diffusive Usadel equation to be

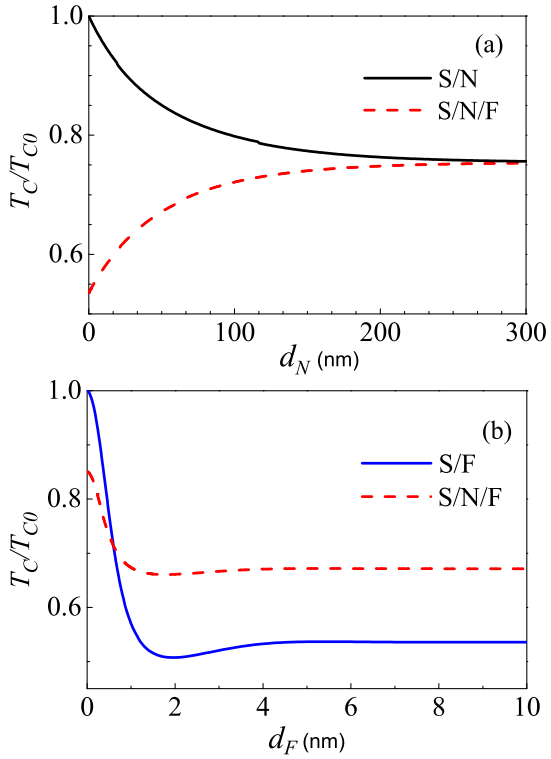

FIG. 2: (a) Numerical results of T_c/T_{c0} of S/N/F and S/N as a function of d_N, shown by dashed and solid curves, respectively. Both curves have the coherence length ξ_N and merge as $d_N \to \infty$ as expected. (b) T_c/T_{c0} of S/N/F and S/F as a function of d_F, shown by the dashed and solid curves. Note the different length scales ξ_N and ξ_{ex} between (a) and (b).

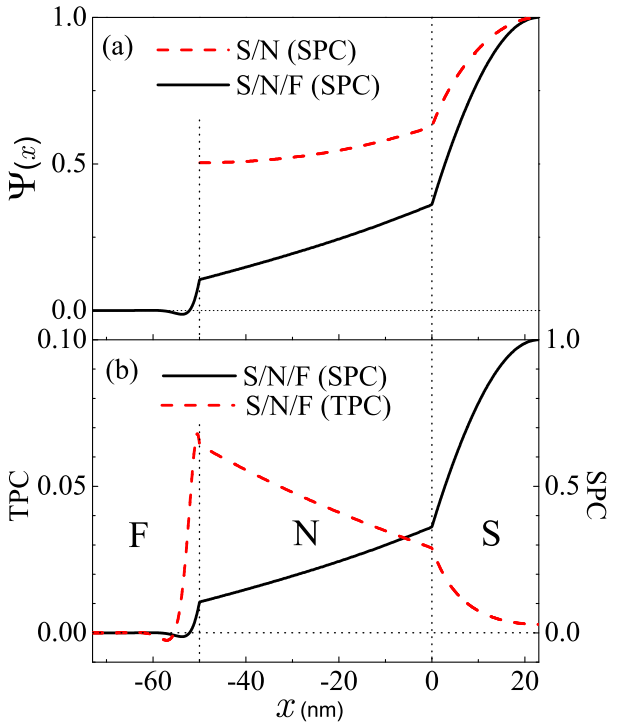

FIG. 3: (a) SPC of S/N/F and S/N shown by the solid and dashed lines, respectively. $\Psi(x)$ is normalized by the value at the outer surface of the S layer. (b) SPC and TPC of an S/N/F trilayer shown by solid and dashed lines, respectively. TPC is magnified by 10 times for clarity.

applicable. Using $D = \frac{1}{3}v_F^2\tau$, and the ξ_F and T_{c0} values, we obtain $E_{ex}\tau \approx 10^{-2}$ so that the Usadel equation is applicable to Nb/CoFe systems.

We show in Fig. 2(a) T_c as a function of N layer thickness, d_N, for $d_S = 23$ nm and $d_F = 23$ nm S/N and S/N/F. For S/N bilayers $T_c(d_N)$ decreases as d_N is increased, but for S/N/F trilayers $T_c(d_N)$ increases as d_N is increased. The length scale of both decrease and increase is given by the N coherence length ξ_N. As $d_N \to \infty$ the two T_c approach each other as expected. In Fig. 2(b) we show T_c as a function of d_F for S/F and S/N/F. Note the different length scales between (a) and (b) given by ξ_N and ξ_{ex}, respectively. $T_c(d_F)$ for S/F shows the well known behavior of an exponential decrease with a shallow dip. For S/N/F, we took $d_N = 50$ nm. The presence of the N layer weakens the effects of exchange energy of F. Consequently, $T_c(d_F)$ for S/N/F, compared with S/F, is lower at $d_F = 0$ but higher as $d_F \to \infty$, and has a shallower dip.

We may also calculate the pair functions as well as T_c from the Usadel equation for various S-N-F layers. In Fig. 3(a) we show the SPC $\Psi^+(x)$ for S/N and S/N/F for $d_S = 23$ nm, $d_N = 50$ nm, and $d_F = 23$ nm, normalized by the value at $x = 23$ nm. It decreases monotonically in N but non-monotonically in F. The non-monotonicity of $\Psi^+(x)$ and $T_c(d_F)$ results from the same physics. It may be understood as originating from the non-zero net momentum of a Cooper pair.[5] In (b) we show both SPC and TPC for an S/N/F. While SPC is maximum at the S outer surface of $x = 23$ nm, TPC is maximum near the N/F interface. The position of TPC peak is roughly ξ_{ex} from the N/F interface.

To see the TPC more clearly, we plot in Fig. 4 the SPC and TCP of S/F bilayers for several values of E_{ex}. Note that for $E_{ex} = 0$ F becomes like an N; the length scale ξ_{ex} becomes ξ_F and TPC vanishes. The TPC becomes small also for large E_{ex} because TPC decays rapidly for small $\xi_{ex} \propto E_{ex}^{-1/2}$. The TPC $\to 0$ as $E_{ex} \to 0$ or $\to \infty$, and is fully induced for an intermediate E_{ex}, as can be seen from figure (b). For each E_{ex}, the peak of TPC is determined by the competition between the exponential decrease of length scale ξ_{ex} and linear increase determined by the BC

$$\xi_S \frac{d}{dx}\mathbf{F}_S(0) - \gamma_{SF}\xi_F \frac{d}{dx}\mathbf{F}_F(0) = 0. \qquad (51)$$

The TPC, therefore, has a peak at around ξ_{ex} away from S/F interface, which can be seen from Fig. 4.

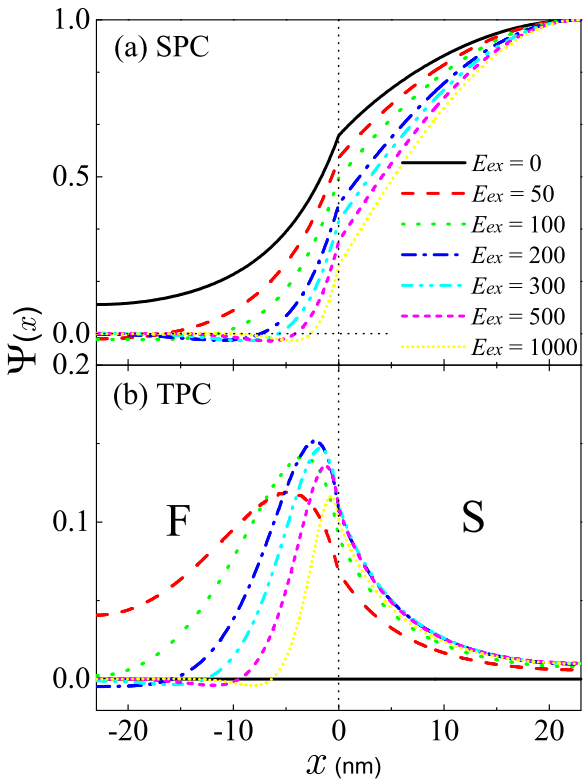

FIG. 4: SPC and TPC of S/F bilayers for several E_{ex}. The peak position of TPC is given by the decay length scale ξ_{ex} of SPC. Note that the TPC vanishes as F becomes an N ($E_{ex} = 0$.

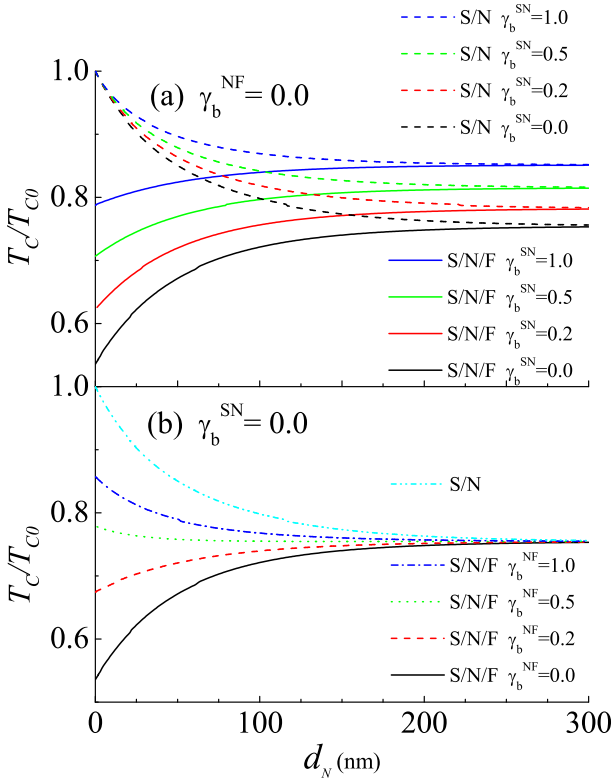

FIG. 5: $T_c(d_N)$ of S/N/F and S/N for several different interface resistances. (a) is for several γ_b^{SN} with $\gamma_b^{NF} = 0$. Two $T_c(d_N)$ curves of S/N/F and S/N merge as $d_N \to \infty$. (b) is for several γ_b^{NF} with $\gamma_b^{SN} = 0$. Note that for small γ_b^{NF} T_c increases as d_N is increased but decreases for large γ_b^{NF}.

B. Effects of interface resistances

We now turn to the more realistic case with non-zero interface resistances. There are two interfaces in an S/N/F, between S and N, and N and F, parameterized by γ_b^{SN} and γ_b^{NF}, respectively. The main effect of the interface resistances is to weaken the proximity effects and increase the T_c of S/N/F trilayers. This can be seen from Fig. 5. Figure (a) shows T_c vs. d_N of S/N/F for several γ_b^{SN} with $\gamma_b^{NF} = 0$. T_c vs. d_N of S/N with the same γ_b^{SN} are also shown for comparison. Figure (b) shows T_c vs. d_N for several γ_b^{NF} with $\gamma_b^{SN} = 0$. In both figures (a) and (b), T_c of a given d_N increases as γ_b is increased.

Another, perhaps more technical, way of saying this is from BC of Eqs. (11), (12), (13), and (14). Non-zero γ_b^{SN} (γ_b^{NF}) introduces the discontinuity of the anomalous function $F^{\pm}$ at the interface. The anomalous function F^{+} and pair function Ψ^{+}, therefore, increases in S but decreases in F region as shown in Figs. 6 and 7. An increase of $\Psi^{+}(x)$ in S means an increase of T_c because it is the largest value of $\Psi^{+}(x)$ that determines T_c. (In the figures, however, $\Psi^{+}(x)$ is normalized at $x = d_S$ and this point is not manifested clearly.) We plot in Fig. 6 $\Psi^{\pm}(x)$ for S/N/F for several γ_b^{SN} values with $\gamma_b^{NF} = 0$. And in Fig. 7 $\Psi^{\pm}(x)$ for several γ_b^{NF} values with $\gamma_b^{SN} = 0$. Note that $\Psi^{+}(x)$ in S region is increased as γ_b^{SN} or γ_b^{NF} is increased.

Now, let us look at in more detail how T_c behaves as a function of d_N for non-zero γ_b^{SN} or γ_b^{NF}. When $\gamma_b^{NF} = 0$ and γ_b^{SN} is increased for S/N/F, as shown in Fig. 5(a), T_c always increases as d_N is increased. However, when γ_b^{NF} is increased with $\gamma_b^{SN} = 0$, $T_c(d_N)$ as a function of d_N behaves somewhat differently. For instance, let us compare the two $T_c(d_N)$ curves for $\gamma_b^{NF} = 0$ and $\gamma_b^{NF} = 1.0$. $T_c(d_N)$ increases with d_N for $\gamma_b^{NF} = 0$ but decreases for $\gamma_b^{NF} = 1.0$, and the two curves merge together as $d_N \to \infty$. This is simple to understand. When $\gamma_b^{NF} = 0.0$, the pair breaking effects of the exchange field of F fully influences S for small d_N, and its effect is weakened as d_N is increased. T_c, therefore, increases as d_N is increased. When $\gamma_b^{NF} = 1.0$, on the other hand, the effects of F is almost blocked out and it behaves like S/N. Consequently, T_c of $\gamma_b^{NF} = 1.0$ is much larger compared with that of $\gamma_b^{NF} = 0.0$ as $d_N \to 0$ and decreases as d_N is

increased. When $d_N \gtrsim 200$ nm, the effects of F are also blocked out irrespective of γ_b^{NF}, and all T_c curves merge together.

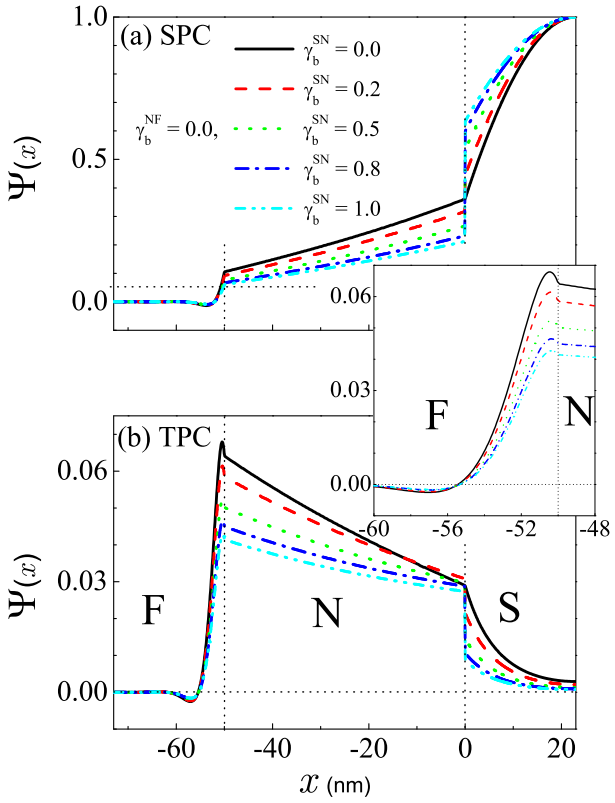

FIG. 6: The SPC and TPC of S/N/F for several γ_b^{SN} with $\gamma_b^{NF} = 0$. The inset shows TPC in detail in F region. Non-zero γ_b^{SN} produces a discontinuity in SPC and TPC at the S/N interface.

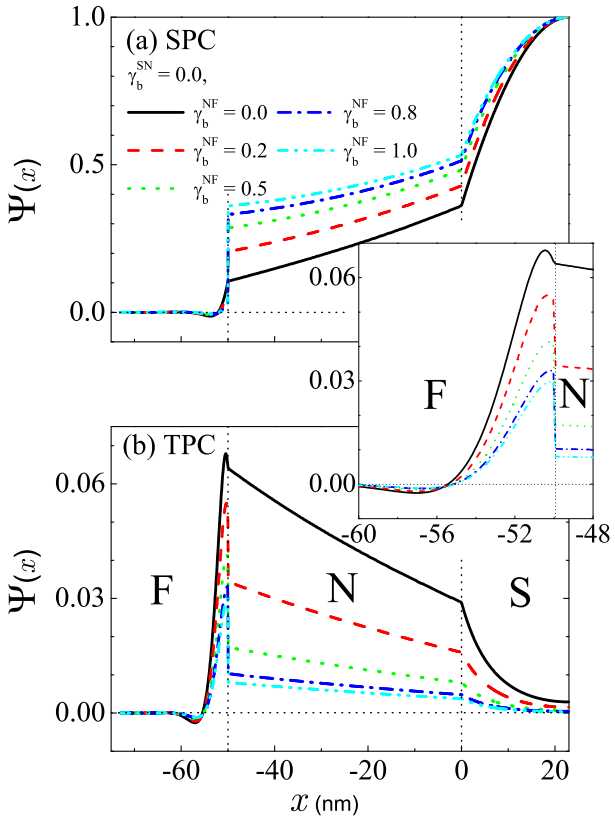

FIG. 7: The SPC and TPC of S/N/F for several γ_b^{NF} with $\gamma_b^{SN} = 0$. The inset shows the TPC in detail in F region. Non-zero γ_b^{NF} introduces the discontinuity at the N/F interface. The TPC in F region is suppressed by γ_b^{NF} less than SPC in F region or TPC in N region.

We now turn to the calculations of pair functions for S/N/F. In Fig. 6 we took $\gamma_b^{NF} = 0$ and plot SPC and TPC for several γ_b^{SN}. Non-zero γ_b^{SN} introduces the discontinuity in both SPC and TPC. The inset shows the peak and dip structure of TPC more closely. As discussed for Fig. 4, the TPC has a peak around ξ_{ex} away from the N/F interface. In Fig. 7 we plot SPC and TPC for several γ_b^{NF} with $\gamma_b^{SN} = 0$. The discontinuity is at the N/F interface in this case.

C. T_c discontinuity due to boundary condition mismatch

An interesting point for $T_c(d_N)$ of S/N/F trilayers appears when we consider $d_N \to 0$ limit. T_c of this limit, of course, ought to coincide with that of the corresponding S/F of $d_N = 0$. For example, T_c of Nb/Au/CoFe trilayers must approach that of Nb/CoFe as Au thickness goes to 0. Also, the change of T_c with d_N should have the length scale of ξ_N simply because there is no other length scale in the N region. We therefore expect that $T_c(d_N)$ of Nb/Au/CoFe trilayers should behave like the curve shown by the long dashed line beginning with the T_c of Nb/CoFe represented by the solid square at the low left corner of the main plot in Fig. 8. The experimental $T_c(d_N)$ measurements, however, show quite different behavior as shown by the solid squares reproduced in Fig. 8.[23] There is an abrupt increase of T_c with the length scale of approximately 2 nm as d_N is increased as shown in the inset, and T_c increases with the expected length scale ξ_N as d_N is further increased.

One may understand this experimental T_c vs. d_N behavior as follows. Recall that in the present formalism the interfaces are modeled in terms of the two parameters γ_b^{SN} and γ_b^{NF} irrespective of N thickness. S/N/F trilayers, as $d_N \to 0$, still have two interfaces characterized by γ_b^{SN} and γ_b^{NF}, but the corresponding S/F bilayer has one interface characterized by γ_b^{SF}. Unless the three γ_bs satisfy a special match condition, $T_c(d_N = 0)$ of the bilayer and $\lim_{d_N \to 0} T_c(d_N)$ of the trilayers need not be

the same. This condition may be derived from the BC of Eqs. (11), (13), and (14). We add (13) and (14), and take $d_N \to 0$. We then obtain using (11)

$$\mathbf{F}_S(0) - \mathbf{F}_F(0) = \left(\gamma_b^{NF} + \gamma_b^{SN}\gamma_{NF}\right)\xi_F \frac{d}{dx}\mathbf{F}_F(0). \quad (52)$$

For this to agree with the corresponding S/F bilayer, it is required that

$$\gamma_b^{SF} = \gamma_b^{NF} + \gamma_b^{SN}\gamma_{NF}. \quad (53)$$

This condition need not be satisfied. The γ_b^{SF} may take an arbitrary value irrespective of γ_b^{NF} or γ_b^{SN}. In case of a mismatch, $T_c(d_N)$ then shows a discontinuity at $d_N = 0$. The right hand side is usually larger as is the case with the Nb/Au/CoFe trilayers, and T_c of $d_N \to 0$ S/N/F should be larger than that of S/F.

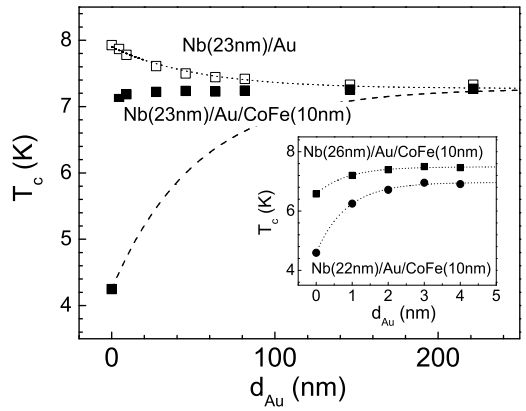

FIG. 8: $T_c(d_N)$ of Nb/Au/CoFe trilayers and Nb/Au bilayers, represented by the solid and empty squares, respectively. Nb and CoFe layers are fixed at $d_S = 23$ and $d_F = 10$ nm. The inset is the detailed plot of the short length scale. The long dashed curve in the main plot is the expected behavior of $T_c(d_N)$ without the BC mismatch. The dotted line connecting empty squares is a guide to eyes. Reproduced from the reference 23.

Note, however, that in experiments $d_N \to 0$ has a single interface of course, and T_c of Nb/Au/CoFe as $d_N \to 0$ must agree with that of Nb/CoFe. As d_N is increased from 0 in Nb/Au/CoFe, there begin to form two distinct interfaces. For the electrons to feel the two interfaces as the theoretical model assumed, a finite width of N region is necessary. This width of about 2 nm is the length which is needed to interpolate the T_c of Nb/CoFe and that of $d_N \to 0$ Nb/Au/CoFe. The theoretical step function behavior of $T_c(d_N)$ then should appear as a short length scale of $\approx$ 2 nm observed in the experiments.[23] This length scale is not the material width of the Nb/Au interface which is approximately an order of magnitude smaller. The same short length of $\approx$ 2 nm has also been observed for N = Cu,[30] Al.[31] The sudden increase of $T_c(d_N)$ as d_N is increased was also observed in the epitaxial Nb(110)/Au(111)/Fe(110) trilayers by Yamazaki and his coworkers.[32]

IV. SUMMARY AND CONCLUDING REMARKS

In this paper, we have extended the Green's function method developed for S/F bilayers by Fominov *et al.* to S/N/F trilayer systems. We have calculated the superconducting transition temperature T_c and the singlet and triplet pairing components near $T \approx T_c$ for S/N/F trilayers. The interface between S and N (N and F) was modeled in terms of γ_b^{SN} (γ_b^{NF}). They represent spin independent interface resistances. As have been and will be reported separately, the experimental T_c measurements could be fit by the present formalism.[23,29,30,31]

There seems, however, a room to improve the present formalism. One possible route might be to model the N/F interface with two spin dependent parameters as was done for example in ref. 27, or to model it in terms of a spin-active interface.[18,19,20,21] The latter route will be an interesting problem in connection with the long range odd frequency triplet pairing components because they are induced even when the exchange field in F region is uniform if the N/F interface in spin-active.

Also noteworthy in the S/N/F system is the observation of the length scale of $\approx$ 20 nm in the T_c vs. d_N measurements in Nb/Au/CoFe trilayers.[23] The natural length scale in N region is the coherence length $\xi_N \approx 100$ nm as shown, for instance, in Figs. 5 and 8. In addition, the short length of $\approx$ 2 nm was observed because of the boundary condition mismatch. In the same experiments the T_c as a function of d_N also exhibited a small oscillation with the length scale of $\approx$ 20 nm. The origin of this is not clear. It seems difficult to understand this oscillation within the current Usadel formalism because there is only one length scale of ξ_N in the theory. It is interesting that this T_c oscillation was also observed in the epitaxial Nb(110)/Au(111)/Fe(110) trilayers.[32] In the epitaxially grown Nb(110)/Au(111)/Fe(110) trilayers the T_c oscillation length scale was $\approx$ 2 nm, which is an order of magnitude smaller than that of the sputtering grown Nb/Au/CoFe trilayers. More experiments with different conditions will be necessary to clarify the origin of the T_c oscillations as a function of d_N.

We have calculated the singlet pairing component and short range odd frequency triplet pairing components in the present paper. The triplet pairing component is induced on top of the dominant singlet component by the proximity effects and time reversal symmetry breaking exchange field. In the present work, the exchange field is unidirectional over the F region, and only the short range triplet component was induced. If the orientation of the exchange field changes in the F region, or if the inner-interface of F is spin active, then the other long range triplet components will also appear. In the latter

case the procedures developed in the present manuscript can be directly applied to understand the long range odd frequency triplet components. We are currently investigating the spectroscopic properties of them in various trilayers of superconductor and ferromagnet where the present formalism can be applied.

Acknowledgments

This work was supported by Korea Science & Engineering Foundation (KOSEF) through Basic Research Program Grant No. R01-2006-000-11248-0 (NYL, HYC, KC) and No. R01-2005-000-10352-0 (HWL) and through SRC program Grant CSCMR (KC) and No. R11-2000-071 (HWL) and by Korea Research Foundation (KRF) through Grant No. KRF-2005-070-C00044 (NYL, HYC) and No. KRF-2005-070-C00055 (HWL), and through BK21 Program (NYL, HYC, KC, HWL).

V. APPENDIX: CALCULATION OF SINGLET AND TRIPLET PAIR FUNCTIONS

We will in this Appendix present the procedure to calculate the singlet and triplet pair functions using the Usadel formalism developed in Sec. II. As discussed there, the anomalous function $\mathbf{F}_S(x,i\omega_n)$ in the S region can be written as

$$\begin{pmatrix} F_S^+(x,i\omega_n) \\ F_S^-(x,i\omega_n) \end{pmatrix} = \begin{pmatrix} F_S^+(x,i\omega_n) \\ C_S^-(i\omega_n)\cosh k_S(x-d_S) \end{pmatrix}. \quad (54)$$

The BC at $x=0$ in terms of $\mathbf{F}_S$ alone is given by Eq. (31).

$$\xi_S \frac{d\mathbf{F}_S(0)}{dx} = \hat{A}_S \mathbf{F}_S(0). \quad (55)$$

We also have

$$\xi_S \frac{d\mathbf{F}_S(0)}{dx} = \hat{A} \mathbf{F}_S(0), \quad (56)$$

where

$$\hat{A} = \begin{pmatrix} W(i\omega_n) & 0 \\ 0 & -A_S \end{pmatrix}, \quad (57)$$

where $W(\omega_n)$ and A_S are given by Eq. (37). We therefore write

$$(\hat{A}_s - \hat{A}) \begin{bmatrix} F_S^+(0,i\omega_n) \\ C_S^-(i\omega_n)\cosh k_S d_S \end{bmatrix} = 0. \quad (58)$$

Dividing this by F_S^+, we obtain

$$\hat{A}_s \begin{bmatrix} 1 \\ 0 \end{bmatrix} = \left(\begin{bmatrix} 1 & 0 \\ 0 & -k_S\xi_S \sinh k_S d_S \end{bmatrix} - \hat{A}_s \begin{bmatrix} 0 & 0 \\ 0 & \cosh k_S d_S \end{bmatrix} \right) \begin{bmatrix} W(i\omega_n) \\ C_S^-(i\omega_n)/F_S^+(0,i\omega_n) \end{bmatrix}. \quad (59)$$

Note that $\Delta(x)$ is the eigenvector corresponding to the smallest eigenvector $M(x,y)$ of Eq. (49), and $F_S^+(x,i\omega_n)$ can be obtained from Eq. (47). We can therefore find $C_S^-(i\omega_n)$ from Eq. (59), and calculate $F_S^-(s,i\omega_n)$ using Eq. (34). This completes the calculation of the SPC and TPC in the S region.

We now turn to calculation of the pairing functions in the N region. The function $F_N^\pm$ can be written as

$$F_N^\pm(x,i\omega_n) = F_N^\pm(0,i\omega_n)\cosh k_N x + \xi_N \frac{d}{dx} F_N^\pm(0,i\omega_n) \frac{\sinh k_N x}{\xi_N k_N}. \quad (60)$$

From the BC (12), we get

$$F_N^\pm(x) = F_S^\pm(0) \left[(1 - \frac{\gamma_b^{SN}}{\gamma_{SN}} \hat{A}_S) \cosh k_N x + \frac{1}{\gamma_{SN}} \hat{A}_S \frac{\sinh k_N x}{\xi_N k_N} \right]. \quad (61)$$

Therefore we get

$$\begin{aligned} F_N^\pm(-d_N) &= F_S^\pm(0) \left[(1 - \frac{\gamma_b^{SN}}{\gamma_{SN}} \hat{A}_S) \cosh k_N d_N - \frac{1}{\gamma_{SN}} \hat{A}_S \frac{\sinh k_N d_N}{\xi_N k_N} \right], \\ \xi_N \frac{d}{dx} F_N^\pm(-d_N) &= F_S^\pm(0) \left[\frac{1}{\gamma_{SN}} \hat{A}_S \cosh k_N d_N - \xi_N k_N (1 - \frac{\gamma_b^{SN}}{\gamma_{SN}} \hat{A}_S) \sinh k_N d_N \right] \end{aligned} \quad (62)$$

$F_N^\pm(-d_N)$ and $\frac{d}{dx}F_N^\pm(-d_N)$ is expressed as $F_S^\pm(0)$ and the results of equation (59) is used together, we can get $F_N^\pm(x)$.

Next, we calculate $F_F^\pm(x)$ in F. The function $F_F^\pm(x)$ is written as Eq. (18). We then use the BC (11) to write

$$\xi_N \frac{d}{dx} F_N^+(-d_N) = \gamma_{NF}\xi_F \left(k_F C_F^+ \sinh k_F d_F + k_F^* C_F^- \sinh k_F^* d_F \right), \quad (63)$$

$$\xi_N \frac{d}{dx} F_N^-(-d_N) = \gamma_{NF}\xi_F \left(-k_F C_F^+ \sinh k_F d_F + k_F^* C_F^- \sinh k_F^* d_F \right) \quad (64)$$

We subtract and add (63) and (64) to obtain

$$C_F^+ = \frac{\xi_N \frac{d}{dx} F_N^+(-d_N) - \xi_N \frac{d}{dx} F_N^-(-d_N)}{2\gamma_{NF}\xi_F k_F \sinh k_F d_F}, \quad (65)$$

$$C_F^- = \frac{\xi_N \frac{d}{dx} F_N^+(-d_N) + \xi_N \frac{d}{dx} F_N^-(-d_N)}{2\gamma_{NF}\xi_F k_F^* \sinh k_F^* d_F}. \quad (66)$$

We then obtain $F_F^\pm$ by plugging $C_F^\pm$ into Eq. (18).

$$F_F^+(x,i\omega_n) = \mathrm{Re} \left[\frac{\xi_N \frac{d}{dx} F_N^+(-d_N) - \xi_N \frac{d}{dx} F_N^-(-d_N)}{2\gamma_{NF}\xi_F k_F \tanh k_F d_F} \right.$$

$$(\cosh k_F(x+d_N)+\sinh k_F(x+d_N)\tanh k_F d_F)\Big], \quad (67)$$

$$F_F^-(x,i\omega_n) = -\mathrm{Im}\left[\frac{\xi_N \frac{d}{dx}F_N^+(-d_N) - \xi_N \frac{d}{dx}F_N^-(-d_N)}{2\gamma_{NF}\xi_F k_F \tanh k_F d_F}\right.$$

$$\left.(\cosh k_F(x+d_N)+\sinh k_F(x+d_N)\tanh k_F d_F)\right]. \quad (68)$$

We can therefore calculate the anomalous functions F in trilayers. The pair functions $\Psi(x)$ are given by

$$\Psi^{\pm}(x) = \pi T_c \sum_{\omega_n>0} F^{\pm}(x,i\omega_n). \quad (69)$$

This completes the calculation of the singlet and triplet pairing components over the entire region of an S/N/F trilayer.

[1] P. G. de Gennes, Rev. Mod. Phys. (1964).
[2] G. Deutscher and P. G. de Gennes, "Proximity effects" in *Superconductivity*, edited by R. D. Parks, p. 1005 (Dekker, New York, 1969).
[3] A. I. Buzdin, Rev. Mod. Phys. **77**, 935 (2005).
[4] F. S. Bergeret, A. F. Volkov, and K. B. Efetov, Rev. Mod. Phys. **77**, 1321 (2005).
[5] E. A. Demler, G. B. Arnold, and M. R. Beasley, Phys. Rev. B **55**, 15174 (1997).
[6] T. Kontos, M. Aprili, J. Lesueur, and X. Grison, Phys. Rev. Lett. **86**, 304 (2001).
[7] V. V. Ryazanov, V. A. Oboznov, A. Yu. Rusanov, A. V. Veretennikov, A. A. Golubov, and J. Aarts, Phys. Rev. Lett. **86**, 2427 (2001).
[8] T. Kontos, M. Aprili, J. Lesueur, F. Genet, B. Stephanidis, and R. Boursier, Phys. Rev. Lett. **89**, 137007 (2002).
[9] W. Guichard, M. Aprili, O. Bourgeois, T. Kontos, J. Lesueur, and P. Gandit, Phys. Rev. Lett. **90**, 167001 (2003).
[10] A. P. Mackenzie and Y. Maeno, Rev. Mod. Phys. **75**, 657 (2003).
[11] V. L. Berezinskii, JETP Lett. **20**, 287 (1975).
[12] V. T. Petrashov, I. A. Sosnin, I. Cox, A. Parsons, and C. Troadec, Phys. Rev. Lett. **83**, 003281 (1999).
[13] M. Giroud, H. Courtois, K. Hasselbach, D. Mailly, and B. Pannetier, Phys. Rev. B 58, R11872 (1998).
[14] F. S. Bergeret, A. F. Volkov, and K. B. Efetov, Phys. Rev. Lett. **86**, 4096 (2001).
[15] T. Champel and M. Eschrig, Phys. Rev. B **72**, 054523 (2005).
[16] R. S. Keizer, S. T. B. Goennenwein, T. M. Klapwijk, G. Miao, G. Xiao, and A. Gupta, Nature **439**, 825 (2006).
[17] T. Lofwander, T. Champel, J. Durst, and M. Eschrig, Phys. Rev. Lett. **95**, 187003 (2005).
[18] A. Millis, D. Rainer, and J. A. Sauls, Phys. Rev. B **38**, 4504 (1988).
[19] E. Zhao, T. Lofwander, and J. A. Sauls, Phys. Rev. B **70**, 134510 (2004).
[20] A. Cottet and W. Belzig, Phys. Rev. B **72**, 180503(R) (2005).
[21] T. Tokuyasu, J. A. Sauls, and D. Rainer, Phys. Rev. B **38**, 8823 (1988).
[22] Y. V. Fominov, N. M. Chtchelkatchev, and A. A. Golubov, Phys. Rev. B **66**, 014507 (2002.)
[23] J. Kim, Y. J. Doh, K. Char, H. Doh, and H. Y. Choi, Phys. Rev. B **71**, 214519 (2005).
[24] K. D. Usadel, Phys. Rev. Lett. **25**, 507 (1970).
[25] M. Y. Kupriyanov and V. F. Lukichev, Sov. Phys. JETP **67**, 1163 (1988).
[26] A. V. Zaitsev, Sov. Phys. JETP **59**, 1015 (1984).
[27] F. Perez-Willard, J. C. Cuevas, C. Surgers, P. Pfundstein, J. Kopu, M. Eschrig, and H. v. Lohneysen, Phys. Rev. B **69**, 140502(R) (2004).
[28] G. B. Arfken and H. J. Weber, *Mathematical methods for physicists*, 5th edition, Chap. 9.5 Green's function – Eigenfunction expansion, p. 618 (Academic Press, 2001).
[29] J. Kim, J. H. Kwon, K. Char, H. Doh, and H. Y. Choi, Phys. Rev. B **72**, 014518 (2005).
[30] K. Kim, J. Kim, K. Char, H. Doh, and H. Y. Choi, submitted to Phys. Rev. B (2006).
[31] J. Kwon and K. Char, unpublished.
[32] H. Yamazaki, N. Shannon, and H. Takagi, Phys. Rev. B **73**, 094507 (2006).